# Wall-Modeled Large-Eddy Simulations of Turbulent Boundary Layer over a Flat-Plate for Aero-Optical Distortion Analysis



Pedro Castillo and Andreas Gross
Mechanical & Aerospace Engineering Department
New Mexico State University, Las Cruces, NM 88003

Daniel R. Guildenbecher, Nathan E. Miller, and Kyle P. Lynch
Engineering Sciences Center
Sandia National Laboratories, Albuquerque, NM 87185



## Objective

Develop a simulation capability for accurate predictions of the aero-optical distortions caused by hypersonic turbulent boundary layer flows

## Tasks

The following steps were taken to meet the objective:

- Extended Wall-Modeled Large Eddy Simulation (WMLES)
- Validated WMLES aero-optic predictions with reference DNS data and Sandia National Laboratories (SNL) measurements
- Evaluated underlying assumptions of a semi-empirical design model for predicting optical distortions at high Mach numbers

## Simulation Strategy

A system of coupled ordinary differential equations was solved for obtaining the wall shear and wall heat flux. The turbulence subgrid stresses were computed with an LES model by Nicoud et al. (1999). Compared to reference direct numerical simulations (DNS) by Zhang et al. (2018), wall-modeling drastically reduces the computational expense of the simulations.

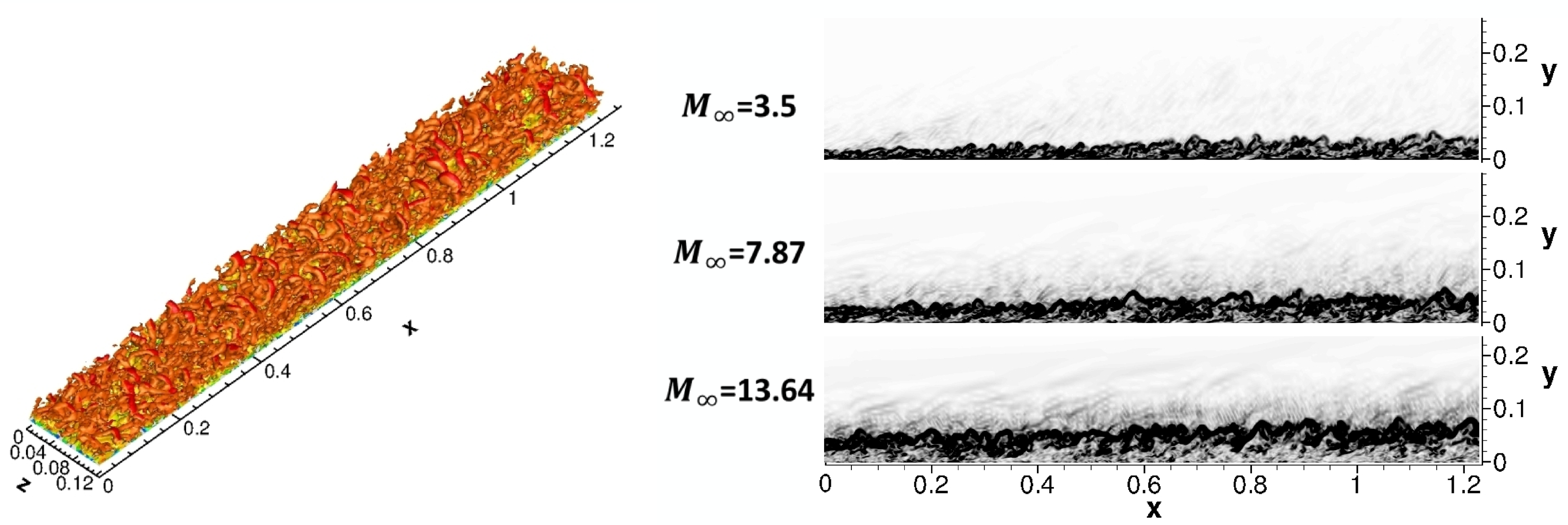


**Figure 1.** Instantaneous $Q$=5 iso-contours for $M_\infty$=7.87 (left) and Numerical Schlieren images (right).

## Computational Grid

The dimensions of the computational grid are 1.2288 x 0.338 x 0.12 in the streamwise, x, wall-normal, y, and spanwise direction, z, respectively. The grid is rectangular with constant grid line spacing in the streamwise and spanwise directions. A grid resolution study was performed for the $M_\infty$=7.87 case to determine the minimum resolution to obtain mean flow profiles and turbulence statistics that reasonably match the reference DNS data. The chosen number of cells in the three directions is 512 x 64 x 160 = $5.24x10^6$ for all three cases.

## Description of cases

The freestream and wall-temperature conditions are summarized in Tab. 1. For the Mach 3.5 case, the conditions of a reference DNS (Barone et al., 2017; Miller et al., 2022) are matched. The Mach 8 case freestream conditions resemble those of the SNL Hypersonic Wind Tunnel (HWT) as reported by Zhang et al. (2018) and Miller et al. (2022). The Mach 14 case is modeled after the AEDC Hypervelocity Tunnel 9 (Zhang et al., 2018). For all cases, the gas behavior was described by the perfect gas state equation. The working gas for Mach 3.5 and 14 was air and the viscosity was obtained from Sutherland's law. The Mach 8 experiment was carried out with nitrogen and the viscosity was calculated with Keyes law.

## Turbulent Statistics

Mean velocity and temperature profiles are plotted in Fig. 2. The dashed parts of the profiles are obtained from the wall model. The WMLES velocity profiles are in excellent agreement with DNS profiles by Zhang et al. (2018) and Miller et al. (2022). The temperature profiles are very similar.

Figure 3 provides a comparison of the fluctuations of the thermodynamic quantities. The density, temperature, and pressure RMS fluctuations were normalized by the local mean density, temperature, and pressure, respectively. The distributions obtained from the WMLES (solid lines) are in adequate qualitative agreement with the reference DNS (dashed lines) (Zhang et al., 2018; Miller et al., 2022).

**Table 1.** Freestream and wall-temperature conditions, and Reynolds numbers.

| $M_\infty$ | $u_\infty$(m/s) | $\rho_\infty(kg/m^3)$ | $T_\infty$(K) | $T_w$(K) | $T_w/T_r$ | $Re_{\theta,in}$ | $Re$ |
|---|---|---|---|---|---|---|---|
| 3.5 | 1144.4 | 0.863450 | 264.9 | Adiabatic | 1.0 | 1907 | $1.60x10^6$ |
| 7.87 | 1154.6 | 0.026018 | 51.8 | 298 | 0.478 | 9714 | $8.16x10^6$ |
| 13.64 | 1882.9 | 0.017001 | 47.4 | 300 | 0.185 | 14408 | $12.0x10^6$ |

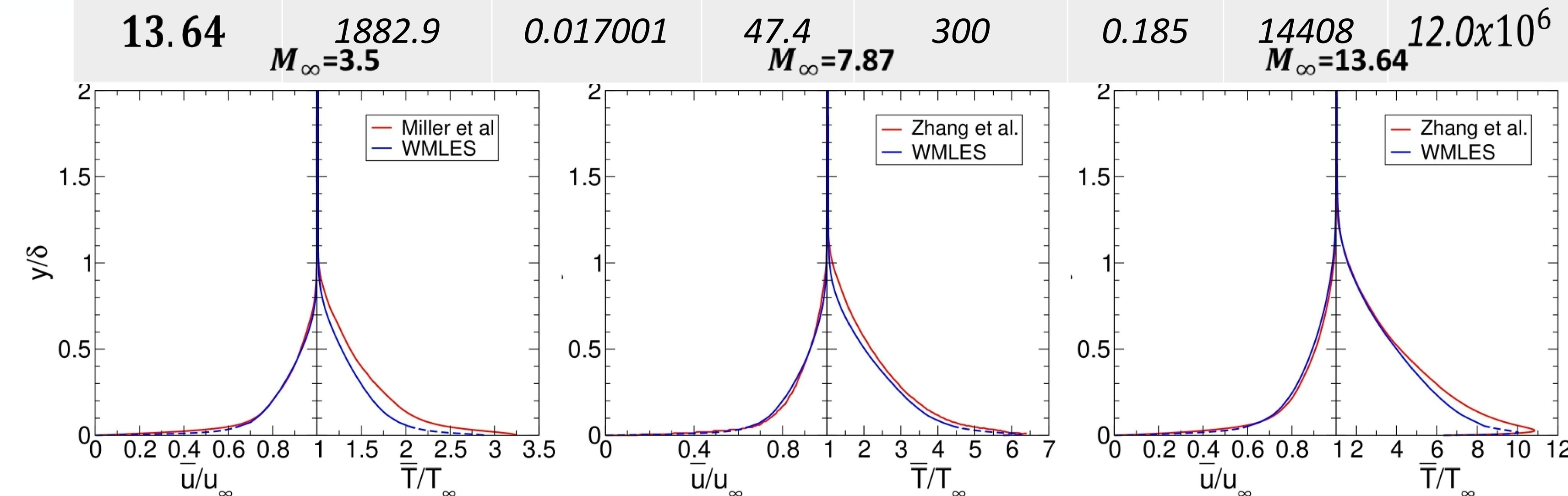


**Figure 2.** Mean velocity and temperature profiles plotted against wall-normal distance.

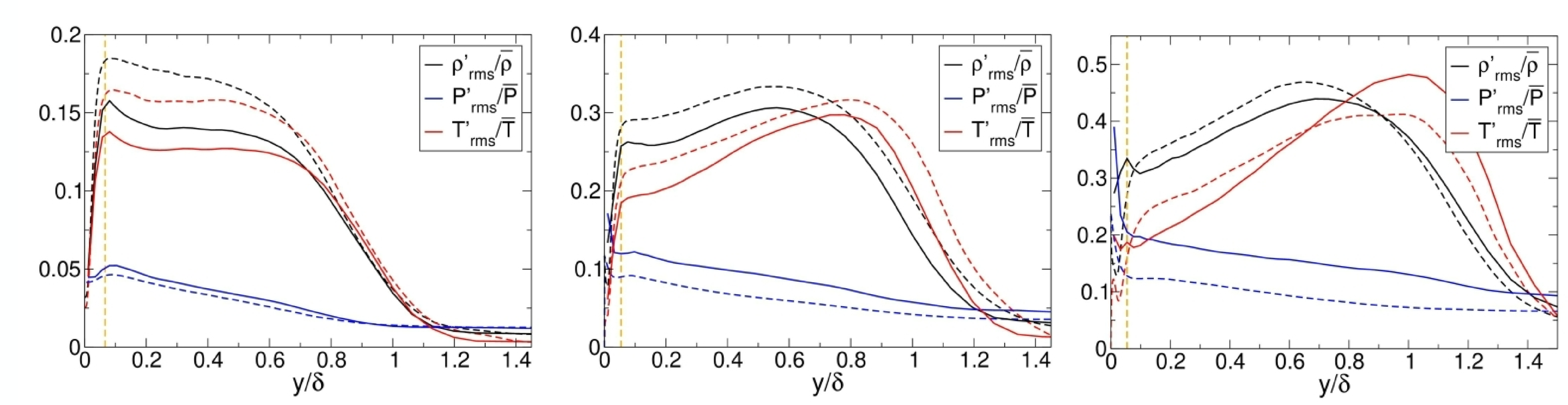


**Figure 3.** Root-mean-square fluctuations of state variables (Solid lines, WMLES; dashed lines, reference DNS).

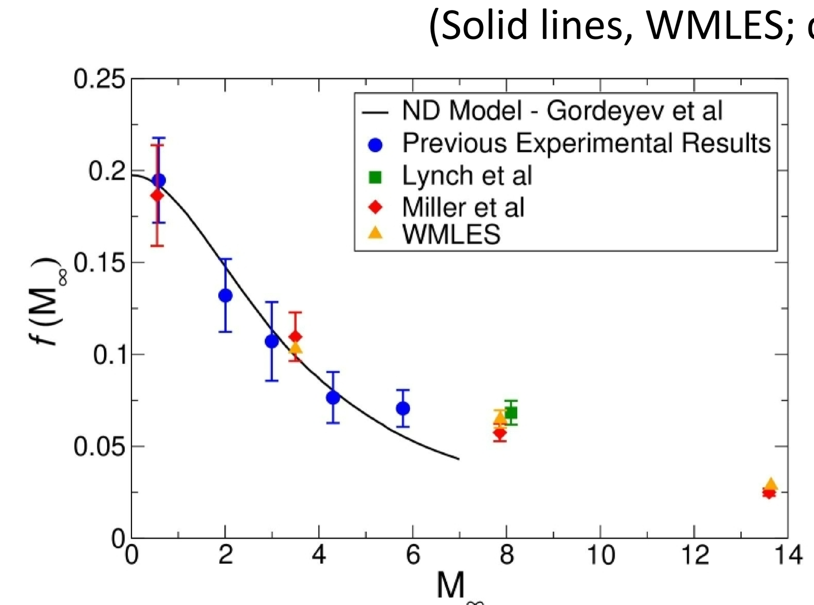


**Figure 4.** Normalized $OPD_{rms}$.

**Table 2.** Normalized $OPD_{rms}$.

| $M_\infty$ | 3.5 | 7.87 | 13.64 |
|---|---|---|---|
| WMLES | 0.1016 | 0.064 | 0.028 |
| DNS | 0.1109 | 0.056 | 0.025 |
| Experiments | -------- | 0.068 | -------- |

## Aero-optics Characterization

The numerical Schlieren images (Fig. 1) indicate regions of strong density gradients. With increasing Mach number, the density gradients are concentrated closer to the boundary layer edge (Fig. 3) and the compressibility effects become more significant. The instantaneous density fields were saved at regular time intervals and the optical path length (OPL) was computed for an aperture with streamwise and spanwise extent of approximately 6δ x 3δ, respectively. A post-processing program was developed to carry out a tilt-tip correction and compute the root-mean-square optical path distortion, $OPD_{rms}$. The normalized $OPD_{rms}$,

$$f(M_\infty) = \frac{OPD_{rms}}{K_{GD}\rho_\infty C_f^{0.5} M_\infty^2 \delta}, \quad (1)$$

obtained from the present WMLES is in good agreement with published data (Fig. 4).

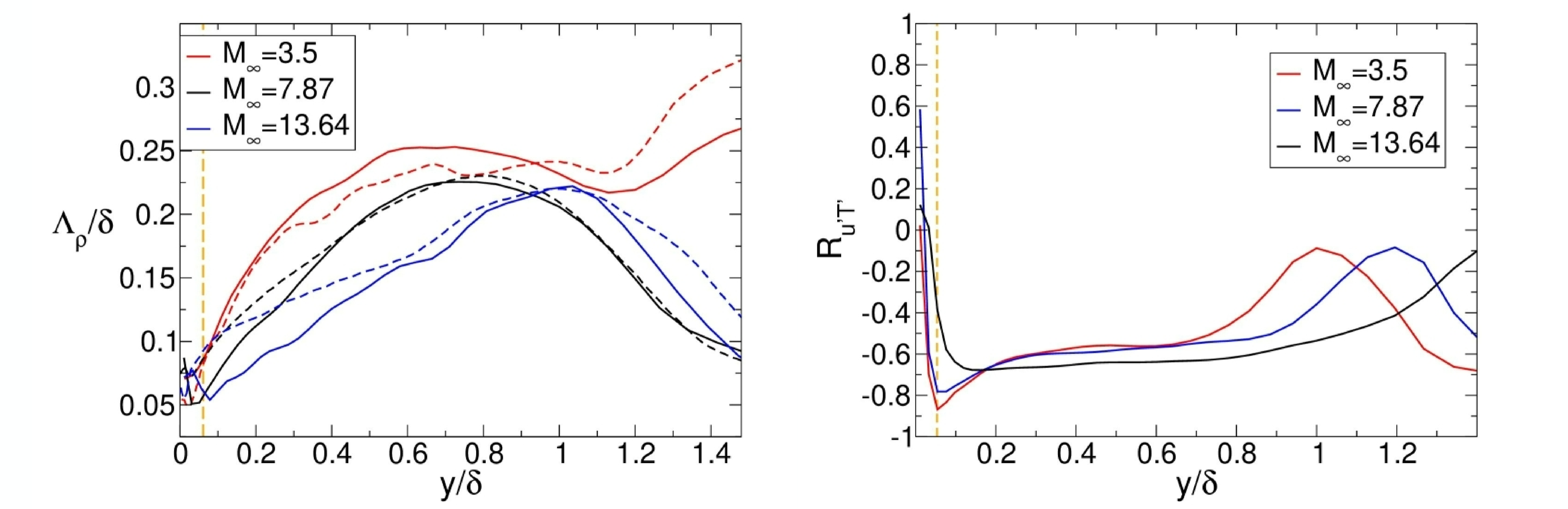


**Figure 5.** Density correlation length (left), and two-point correlation coefficient (right).

## Model Assumptions

The Notre Dame (ND) model (Eqn. 1) by Gordeyev et al (2017) is based on the "linking equation" which requires knowledge of the correlation length of the fluctuating density field in the light propagation direction. Distributions of the correlation length, (Fig. 5) are in good agreement with reference data by Miller et al (2022). As the Mach number increases, the peak of the correlation length moves towards the boundary layer edge.

The Strong Reynolds Analogy (SRA) provides another important underlying foundation for the ND model. The SRA postulates a direct relationship between the momentum exchange and heat transfer. In its simplest form, the temperature and velocity fluctuations are perfectly anti-correlated ($R_{u'T'} = -1$) and temperature fluctuations resulting from pressure or density fluctuations are neglected (Miller et al., 2022). The present simulations reveal that independent of the Mach number, the correlation is approximately $R_{u'T'} = -0.6$ throughout the boundary layer and trending towards zero at the boundary layer edge. Near the wall, the correlation peaks at $R_{u'T'} = -0.8$.

## Conclusions

Wall-modeled large-eddy simulations (WMLES) provides a reasonable low-cost alternative to direct numerical simulations for the prediction of the aero-optical distortions for high-speed boundary layer flows. The present WMLES indicate that the Notre Dame model underpredict the optical path distortion at high Mach numbers. This was attributed to the key underlying assumptions. Future research directed at an extension of the model to high Mach number flows will build on the present results (WMLES, DNS, experiments).

## Publication and References


- Castillo, P., Gross, A., Miller, N.E., Guildenbecher, D.R., and Lynch, K.P., ``Wall-Modeled Large-Eddy Simulations of Turbulent Mach 3.5, 8, and 14 Boundary Layers - Effect of Mach Number on Aero-Optical Distortions," AIAA Paper *AIAA-2022-3441*, 2022.
- Zhang, C., Duan, L., and Choudhari, M.M., ``Direct Numerical Simulation Database for Supersonic and Hypersonic Turbulent Boundary Layers," *AIAA Journal*, Vol. 56, No. 11, 2018, pp. 4297-4311.
- Miller, N.E., Lynch, K.P., Gordeyev, S., Guildenbecher, D.R., Duan, L., and Wagnild, R.M., ``Aero-optical Distortions of Turbulent Boundary Layers: Hypersonic DNS,"AIAA Paper *AIAA-2022-0056*, 2022.
- Jumper, E.J., and Gordeyev, S., ``Physics and Measurement of Aero-Optical Effects: Past and Present," *Annual Review of Fluid Mechanics*, Vol. 49, No. 1, 2017.


## Acknowledgments

The support of the Laboratory Directed Research and Development program at Sandia National Laboratories is gratefully acknowledged. Sandia National Laboratories is a multimission laboratory managed and operated by National Technology and Engineering Solutions of Sandia, LLC, a wholly owned subsidiary of Honeywell International Inc., for the U.S. Department of Energy's National Nuclear Security Administration under contract DE-NA0003525. This poster describes objective technical results and analysis. Any subjective views or opinions that might be expressed in the paper do not necessarily represent the views of the U.S. Department of Energy or the United States Government.